

# Giant spin canting in the $S = 1/2$ antiferromagnetic chain $[\text{CuPM}(\text{NO}_3)_2(\text{H}_2\text{O})_2]_n$ observed by $^{13}\text{C}$ -NMR

A.U.B. Wolter,<sup>1</sup> P. Wzietek,<sup>2</sup> S. Süllow,<sup>1</sup> F.J. Litterst,<sup>1</sup> A. Honecker,<sup>3</sup> W. Brenig,<sup>3</sup> R. Feyerherm,<sup>4</sup> and H.-H. Klauss<sup>1</sup>

<sup>1</sup>*Institut für Metallphysik und Nukleare Festkörperphysik,  
TU Braunschweig, 38106 Braunschweig, Germany*

<sup>2</sup>*Laboratoire de Physique des Solides, Université Paris-Sud, 91405 Orsay*

<sup>3</sup>*Institut für Theoretische Physik, TU Braunschweig, 38106 Braunschweig, Germany*

<sup>4</sup>*Hahn-Meitner-Institut GmbH, 14109 Berlin, Germany*

(Dated: May 23, 2019)

We present a combined experimental and theoretical study on copper pyrimidine dinitrate  $[\text{CuPM}(\text{NO}_3)_2(\text{H}_2\text{O})_2]_n$ , a one-dimensional  $S = 1/2$  antiferromagnet with alternating local symmetry. From the local susceptibility measured by NMR at the three inequivalent carbon sites in the pyrimidine molecule we deduce a giant spin canting, *i.e.*, an additional staggered magnetization perpendicular to the applied external field at low temperatures. The magnitude of the transverse magnetization, the spin canting of  $52^\circ$  at 10 K and 9.3 T and its temperature dependence are in excellent agreement with exact diagonalization calculations.

PACS numbers: 75.50.Ee, 76.60.Cq, 75.10.Jm, 75.50.Xx

One-dimensional quantum magnets show a rich variety of different magnetic ground states, such as spin liquids with quantum critical behavior or gaps in the spin excitation spectrum [1, 2, 3]. The idealized  $S = 1/2$  antiferromagnetic Heisenberg chain ( $S = 1/2$  AFHC) with uniform nearest-neighbor exchange coupling is of particular interest, since it is exactly solvable using the Bethe ansatz equations [4, 5, 6]. Its ground state is a spin singlet with gapless excitations, but small modifications of the model fundamentally change the ground state magnetic properties.

In real spin chain systems such a modification often results from a low symmetry of the crystallographic lattice. The case of an alternating local environment of the magnetic ion can be treated theoretically including the antisymmetric Dzyaloshinskii-Moriya (DM) interaction and/or a staggered  $g$  tensor, both as consequence of the residual spin-orbit coupling [7, 8, 9]. Whereas the Heisenberg exchange  $J\mathbf{S}_i\mathbf{S}_{i+1}$  prefers collinear spin arrangements, the DM interaction of the form  $\mathbf{D}(\mathbf{S}_i \times \mathbf{S}_{i+1})$  prefers canted ones. This can be described by an additional induced staggered field  $h_s$  perpendicular to an applied magnetic field  $H$ . The Hamiltonian is written as [7]

$$\hat{H} = J \sum_i [\mathbf{S}_i \mathbf{S}_{i+1} - h_u S_i^z - (-1)^i h_s S_i^x], \quad (1)$$

with  $J$  as the coupling constant,  $h_u = g\mu_B H/J$  as the effective uniform field and  $h_s \propto H$ . In the following, we refer to this as the *staggered*  $S = 1/2$  AFHC model. An essential result derived from the model is the opening of a spin excitation gap in external applied fields, with the excitation spectrum consisting of solitons, antisolitons and their bound states called breathers [8, 9].

This model has been used to describe several stag-

gered  $S = 1/2$  AFHCs, that is, copper benzoate [2, 9], copper pyrimidine dinitrate  $[\text{CuPM}(\text{NO}_3)_2(\text{H}_2\text{O})_2]_n$  ( $\text{CuPM}$ ) [10, 11, 12] and  $\text{CuCl}_2 \cdot 2(\text{dimethylsulfoxide})$  [13]. However, two of the generic features of this model, *i.e.*, the magnitude and direction of a transverse staggered magnetization  $m_{s\perp}$  and its temperature dependence have not been verified experimentally by now.

In this Letter we report the first direct observation of the staggered magnetization  $m_{s\perp}$  in  $\text{CuPM}$  via a detailed  $^{13}\text{C}$ -NMR study. We compare our data with exact diagonalization calculations based upon the staggered  $S = 1/2$  AFHC model. At 10 K and 9.3 T the transverse magnetization gives rise to a giant spin canting of  $52^\circ$  with respect to the external field. This observation manifests the strong influence of spin orbit coupling in this system.

We measured the local susceptibility via the NMR frequency shift at three inequivalent carbon sites in the pyrimidine molecule as a function of temperature and magnetic field orientation. The transverse staggered magnetization  $m_{s\perp}$  is identified both (*i*) as a low temperature deviation from the linear correlation between local and macroscopic susceptibility and (*ii*) from the orientation dependence of the NMR frequency shift  $\delta$  at a fixed temperature. The observed magnitude ( $m_{s\perp} \approx 0.13 \mu_B$  at 10 K in 9.3 T) and temperature dependence are in excellent agreement with the staggered  $S = 1/2$  AFHC model.

Single crystals of  $[\text{CuPM}(\text{NO}_3)_2(\text{H}_2\text{O})_2]_n$  have been grown as described previously [14]. The Cu ions form uniformly spaced chains running parallel to the short *ac* diagonal of the monoclinic crystal structure. The intrachain magnetic exchange pathway is provided by the pyrimidine ring  $\text{C}_4\text{N}_2\text{H}_4$ , which connects two neighboring Cu ions as shown in Figs. 1 and 2. From a single crystal study of  $[\text{CuPM}(\text{NO}_3)_2(\text{H}_2\text{O})_2]_n$  a magnetic exchange parameter  $J/k_B = 36.3(5)$  K is derived [10, 11]. An ad-

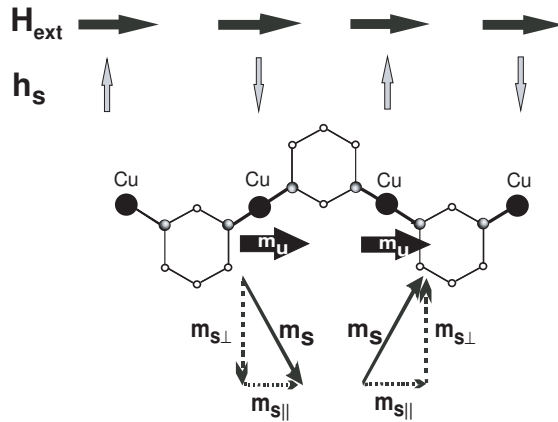


FIG. 1: A chain segment of  $[\text{CuPM}(\text{NO}_3)_2(\text{H}_2\text{O})_2]_n$  viewed along the  $b$ -direction. For clarity, only the Cu ions and the pyrimidine molecules are shown. The directions of the different components to the magnetization, *i.e.*,  $m_u$ ,  $m_s = m_{s\parallel} + m_{s\perp}$ , are illustrated on the middle chain segment. Note that the different staggered components are not to scale.

ditional Curie-like contribution to the magnetic susceptibility at low temperatures is observed. It varies strongly with magnitude and direction of the applied external field and is identified as the longitudinal component  $m_{s\parallel}$  of the total staggered magnetization  $m_s$ . Here, following Refs. [10, 11], with  $m_s$  we denote the magnetization induced by the staggered field which has both a staggered ( $m_{s\perp}$ ) and a uniform ( $m_{s\parallel}$ ) component. In CuPM  $m_{s\parallel}$  is only  $\leq 0.11$  of the total staggered magnetization. The different contributions to the magnetization induced by either the applied external or staggered field are illustrated in Fig. 1.

We have performed NMR experiments using a home-built spectrometer and a superconducting magnet (9.3 T) and temperatures 5-200 K. The single-crystal was oriented with the  $ac$ -plane parallel to the external field. The NMR spectra of  $^{13}\text{C}$  have been recorded using a progressive saturation sequence with constant delay and Hahn spin-echo detection. The  $^{13}\text{C}$  NMR shift  $\delta$  is defined as the normalized difference between the observed resonance frequency  $\omega_{\text{res}}$  and the calculated value for the bare nucleus,  $\delta = \frac{\omega_{\text{res}} - \gamma B_0}{\gamma B_0}$ .  $\gamma$  is the gyromagnetic ratio of the nucleus,  $B_0$  was determined from the  $^1\text{H}$ -NMR resonance frequency of water at room temperature. In  $[\text{CuPM}(\text{NO}_3)_2(\text{H}_2\text{O})_2]_n$ , the three inequivalent carbon sites C1, C2 and C3 with additional hyperfine coupling to the nearest proton ( $I = 1/2$ ) result in three pairs of NMR resonance lines (Fig. 2) [15].

A direct comparison of the NMR shift  $\delta(T)$  with the measured macroscopic susceptibility  $\chi(T)$  is shown in Fig. 3. In this plot each set of hyperfine doublets is represented by its averaged shift.  $\delta$  can be described by

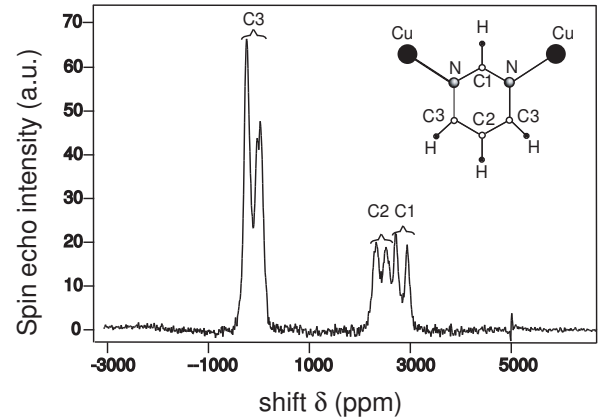


FIG. 2: A typical  $^{13}\text{C}$ -NMR spectrum of  $[\text{CuPM}(\text{NO}_3)_2(\text{H}_2\text{O})_2]_n$  at  $T = 15$  K in an external field of 9.3 T applied along the copper chain direction. The site assignment of the observed signals has been derived from the angular dependent NMR shift  $\delta$  at 200 K [15].

the sum of two contributions: the chemical shift  $\sigma_0$  and the Knight shift  $K$ . While  $\sigma_0$  represents the temperature independent orbital shift due to closed electronic shells, the Knight shift  $K$  describes the hyperfine coupling to the paramagnetic electronic moments mainly residing on the Cu sites. It can be decomposed as  $K(T) = A \cdot \chi(T)$ . Here,  $A$  is the hyperfine coupling constant, which can either have positive or negative sign, and  $\chi(T)$  is the magnetic susceptibility. The solid lines in Fig. 3 represent linear fits of the form  $\delta(T) = \sigma_0 + A \cdot \chi(T)$  for  $T \geq 30$  K. Whereas for  $H \perp$  chain this linear relation is obeyed in the full temperature range (5-120 K), a large deviation is observed below 30 K for  $H \parallel$  chain. In this geometry the transverse component of the staggered magnetization  $m_{s\perp}$  results in an additional Knight shift  $K_s$  [16].

$K_s$  is extracted from the data via  $K_s(T) = \delta(T) - \sigma_0 - A \cdot \chi(T)$  and is shown in Fig. 4 (a) for sites C1, C2 and C3, respectively. The solid lines represent fits to  $K_s(T) = A_{\text{dip},\uparrow\downarrow} \cdot C_s / T + K_{s,\text{corr}}$ . The hyperfine coupling constant for a staggered magnetization along the crystallographic  $b$ -axis,  $A_{\text{dip},\uparrow\downarrow}$ , is calculated in localized dipole approximation within a sphere of 120 Å centered at the respective carbon site. A small offset  $K_{s,\text{corr}} \approx -250$  ppm had to be included since in this analysis the experimental value  $K_s(30\text{K})$  is fixed as zero. The fit parameters  $C_s$  for the three carbon sites result in independent values for  $m_{s\perp}$ , namely  $m_{s\perp}(\text{C1}) = (0.07 \pm 0.01)\mu_B$ ,  $m_{s\perp}(\text{C2}) = (0.16 \pm 0.01)\mu_B$  and  $m_{s\perp}(\text{C3}) = (0.07 \pm 0.01)\mu_B$  at 10 K in 9.3 T external field.

In Fig. 4 (b) we compare the average of the experimental results obtained from the three carbon sites,  $\bar{m}_{s\perp}$ , with results for the uniform  $z$ -component  $m_u$  and the staggered  $x$ -component  $m_s$  of the magnetization obtained by full diagonalization of the  $S = 1/2$  AFHC chain Hamiltonian (1) with  $N = 16$  sites. Here, we have used

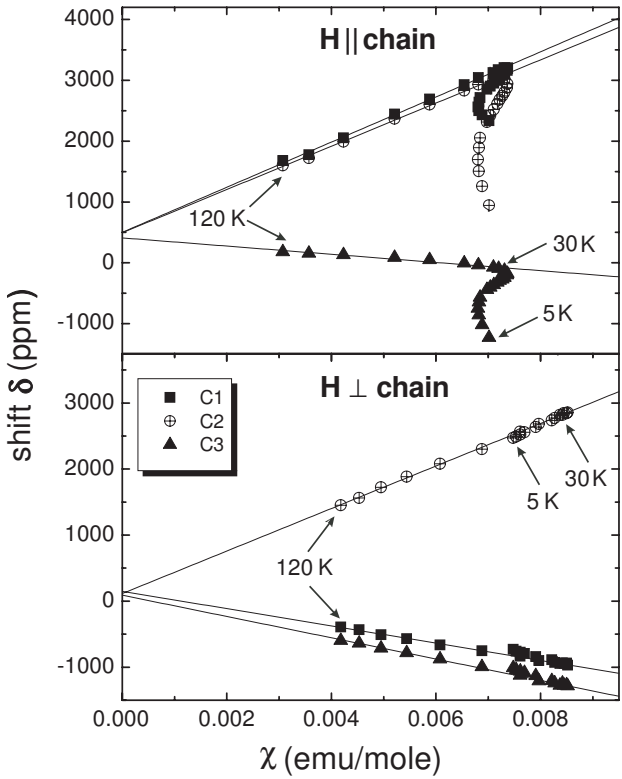


FIG. 3: NMR shifts  $\delta$  vs experimental magnetic susceptibility  $\chi$  for  $[\text{CuPM}(\text{NO}_3)_2(\text{H}_2\text{O})_2]_n$  with the external field  $H \parallel$  and  $\perp$  to the chain in the  $ac$ -plane. The solid lines are fits of the form  $\delta(T) = \sigma_0 + A \cdot \chi(T)$  for  $T \geq 30\text{K}$ .

$J/k_B = 36.5\text{ K}$ , a ratio of the staggered and uniform field  $h_s/h_u = 0.083$  and a  $g$  value of  $g = 2.117$  for  $H \parallel$  chain [10, 11]. Comparison with results for  $N < 16$  (not shown) and for  $N = 20$  at  $T = 0$  [11] indicates that the data for  $N = 16$  yields a good approximation to the thermodynamic limit at all temperatures. We find excellent agreement between experiment and theory in the whole temperature range. At  $10\text{ K}$  and  $9.3\text{ T} \parallel$  chain the ratio of the staggered magnetization,  $m_s = 0.13\ \mu_B$ , to the uniform one,  $m_u = 0.10\ \mu_B$ , corresponds to a giant spin canting of  $52^\circ$  with respect to the external field. With decreasing temperature the spin canting increases, extrapolating to  $\sim 75^\circ$ .

In an independent approach to extract  $m_{s\perp}$  we measured the angular dependence of  $\delta$  in the  $ac$ -plane at  $200\text{ K}$  [15],  $30\text{ K}$  and  $10\text{ K}$  (Fig. 5). We take into account anisotropic dipole and isotropic hyperfine coupling to the longitudinal susceptibility  $\underline{\chi}_u + \underline{\chi}_{s\parallel}$ , anisotropic dipole coupling to the transverse susceptibility  $\underline{\chi}_{s\perp}$ , and the orbital shift  $\underline{\sigma}$ :

$$\delta = \frac{1}{H^2} (\mathbf{H} \cdot \underline{\mathbf{A}}_{dip,\uparrow\downarrow} \cdot (\underline{\chi}_u + \underline{\chi}_{s\parallel}) \cdot \mathbf{H} + A_{iso} \mathbf{H} \cdot (\underline{\chi}_u + \underline{\chi}_{s\parallel}) \cdot \mathbf{H} +$$

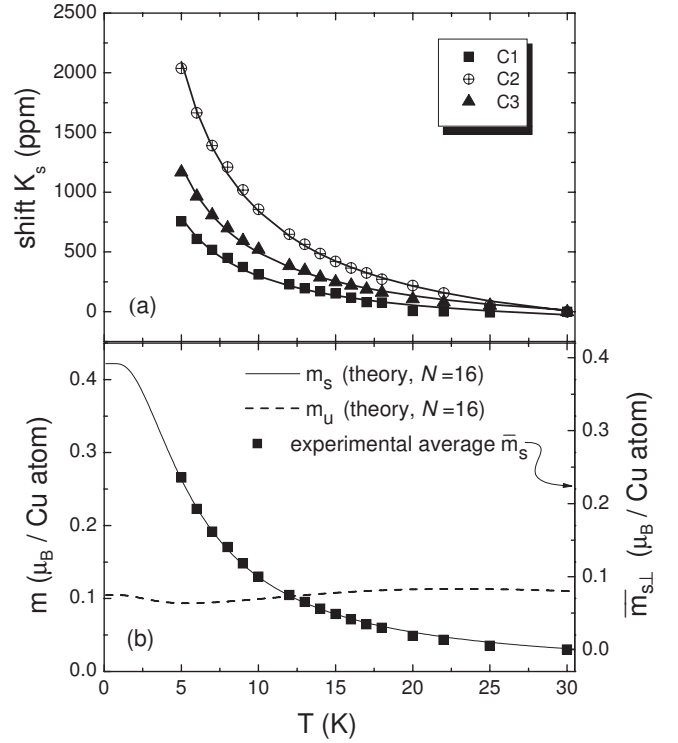


FIG. 4: (a) The temperature dependent transverse staggered contribution to the Knight shift,  $K_s$ , in  $[\text{CuPM}(\text{NO}_3)_2(\text{H}_2\text{O})_2]_n$  with the external field  $H \parallel$  to the Cu chains. The solid lines are a parametrization to  $K_s = A_{dip,\uparrow\downarrow} \cdot C_s / T + K_{s,corr}$ . (b)  $\bar{m}_{s\perp}$ , the experimental average of the three carbon sites, and exact diagonalization calculations of a linear chain with  $N = 16$  spins for both, the staggered magnetization  $m_s$  and  $m_u$ . Note that a small offset ( $-0.02\ \mu_B / \text{Cu atom}$ ) of the magnetization scale for the experimental data  $\bar{m}_{s\perp}$  is necessary due to the data analysis which sets  $K_s(30\text{ K}) = 0$ .

$$+ \mathbf{H} \cdot \underline{\mathbf{A}}_{dip,\uparrow\downarrow} \cdot \underline{\chi}_{s\perp} \cdot \mathbf{H} + \\ + \mathbf{H} \cdot \underline{\sigma} \cdot \mathbf{H}). \quad (2)$$

The dipole hyperfine tensors for uniform and staggered susceptibility,  $\underline{\mathbf{A}}_{dip,\uparrow\uparrow}$  and  $\underline{\mathbf{A}}_{dip,\uparrow\downarrow}$ , are obtained by dipole field calculations taking into account magnetic moments localized mainly at the Cu sites within a sphere of radius  $R = 120\text{ \AA}$  centered at the respective carbon atom. In order to adequately describe the data one needs to take into account a finite moment transfer of 10% to the nitrogen atoms of the pyrimidine molecules in the calculation of  $\underline{\mathbf{A}}_{dip,\uparrow\downarrow}$ . The moment transfer is consistent with preliminary electronic structure calculations [17] and it is close to the value observed in a MnCu antiferromagnetic chain system [18]. We also considered a finite moment transfer to the nitrogen atoms in the calculations of  $\underline{\mathbf{A}}_{dip,\uparrow\downarrow}$ . Here, a 100% transverse moment on the Cu site yields the best description of our data and is used throughout this work. The orbital shift tensor  $\underline{\sigma}$  was calculated from  $\sigma_0$

measured  $\parallel$  and  $\perp$  to the chain [19]. For 30 K the contributions from the staggered susceptibilities,  $\chi_{s\parallel}$  and  $\chi_{s\perp}$ , are nearly zero. Thus, to describe the experimental data at 30 K,  $A_{iso}$  is the only fit parameter and is determined to:  $A_{iso,C1} = (0.05 \pm 0.01)$  mole/emu,  $A_{iso,C2} = (0.38 \pm 0.01)$  mole/emu and  $A_{iso,C3} = (-0.07 \pm 0.01)$  mole/emu.

Using the isotropic constants  $A_{iso}$  determined at  $T = 30$  K and the experimental values for  $\chi_{s\parallel}$  from Ref. [10], the remaining parameter to fit our NMR shift data at 10 K is the transverse staggered susceptibility  $\chi_{s\perp}$ . The solid lines in Fig. 5(b) represent the fits to Eq. (2). We obtain  $m_{s\perp}(C1) = (0.09 \pm 0.01)\mu_B$ ,  $m_{s\perp}(C2) = (0.20 \pm 0.02)\mu_B$  and  $m_{s\perp}(C3) = (0.06 \pm 0.01)\mu_B$  for  $H \parallel$  chain. These values are fully consistent with the results of the analysis of the temperature dependence of  $K_s$ , as presented above. Not incorporating the transverse staggered component  $\mathbf{H} \cdot \mathbf{A}_{dip,\uparrow} \cdot \chi_{s\perp} \cdot \mathbf{H}$  in our description yields an angular dependence of  $\delta$  as indicated by the dashed curves in Fig. 5(b). Clearly, our data are not well reproduced in this case.

We believe that the variance of the results of  $m_{s\perp}$  for the three inequivalent carbon sites stems from the localized dipole approximation which we used to calculate the dipole hyperfine coupling tensors  $\mathbf{A}_{dip}$ . This would indicate that in order to improve the description of our data the effect of delocalization of spin-density ought to be considered by means of extended electronic structure calculations.

In conclusion, we have performed  $^{13}\text{C}$ -NMR experiments on  $[\text{CuPM}(\text{NO}_3)_2 \cdot (\text{H}_2\text{O})_2]_n$  as function of temperature and magnetic field orientation. We extracted the transverse staggered magnetization as a low temperature deviation from the linear correlation between local and global susceptibility, and from the orientation dependence of the NMR frequency shift at 10 K. The observed temperature dependence is in excellent agreement with theoretical results for the staggered  $S = 1/2$  AFHC model. The observed giant spin canting highlights the influence of weak residual spin orbit interactions in such systems. Our data also provide detailed information on the hyperfine coupling in  $[\text{CuPM}(\text{NO}_3)_2 \cdot (\text{H}_2\text{O})_2]_n$  as well as on the absolute value of the staggered magnetization. The remaining small variance between the experimental values  $m_{s\perp}$  for inequivalent carbon sites likely reflects details of the orbital structure of the system, which to resolve will require further electronic structure calculations.

This work has partially been supported by the Deutsche Forschungsgemeinschaft DFG under contract number KL1086/4-2 and the European Community within the framework of the Marie-Curie training fellowship programme STROCOLODI. A.U.B. Wolter would like to thank the Laboratoire de Physique des Solides for hospitality and D. Jérôme for fruitful discussions. The numerical results presented in Fig. 4(b) have been ob-

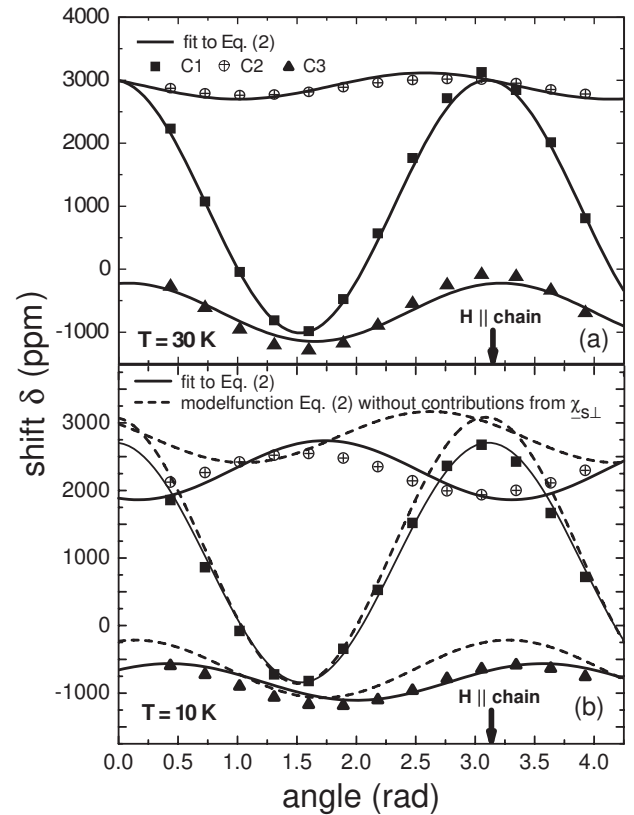


FIG. 5: The angular-dependent NMR shift  $\delta$  of  $[\text{CuPM}(\text{NO}_3)_2 \cdot (\text{H}_2\text{O})_2]_n$  at  $T = 30$  K and 10 K, respectively, with the external field aligned in the  $ac$ -plane. For further details see text.

tained on the compute-server `cfgauss` at the computing center of the TU Braunschweig.

---

- [1] F.D.M. Haldane, Phys. Rev. Lett. **50**, 1153 (1983).
- [2] D.C. Dender *et al.*, Phys. Rev. Lett. **79**, 1750 (1997).
- [3] M.B. Stone *et al.*, Phys. Rev. Lett. **91**, 037205 (2003).
- [4] H.A. Bethe, Z. Phys. **71**, 205 (1931).
- [5] M. Takahashi, *Thermodynamics of One-Dimensional Solvable Models* (Cambridge University Press, Cambridge, 1999).
- [6] A. Klümper and D.C. Johnston, Phys. Rev. Lett. **84**, 4701 (2000).
- [7] M. Oshikawa and I. Affleck, Phys. Rev. Lett. **79**, 2883 (1997); I. Affleck and M. Oshikawa, Phys. Rev. B **60**, 1038 (1999).
- [8] F.H.L. Essler and A.M. Tsvelik, Phys. Rev. B **57**, 10592 (1998); F.H.L. Essler, Phys. Rev. B **59**, 14376 (1999).
- [9] T. Asano *et al.*, Phys. Rev. Lett. **84**, 5880 (2000).
- [10] R. Feyerherm *et al.*, J. Phys.: Condens. Matter **12**, 8495 (2000).
- [11] A.U.B. Wolter *et al.*, Phys. Rev. B **68**, 220406(R) 2003.
- [12] S.A. Zvyagin *et al.*, cond-mat/0403364.

- [13] M. Kenzelmann *et al.*, cond-mat/0305476.
- [14] T. Ishida *et al.*, *Synth. Metals* **85**, 1655 (1997).
- [15] A.U.B. Wolter *et al.*, *Polyhedron* **22**, 2273 (2003).
- [16] Although for  $H \perp$  chain a small transverse staggered magnetization  $m_{s\perp}$  is also present [10], the dipole coupling constant for a transverse spin polarisation is nearly zero in this geometry and thus one cannot detect an additional Knight shift  $K_s$ .
- [17] K. Doll, private communication.
- [18] B. Gillon, *Mol. Cryst. and Liq. Cryst.* **335**, 53 (1999).
- [19] Assuming the principal axes of the orbital shift tensor  $\underline{\underline{\alpha}}$  to be the C-H bond axis, the perpendicular axis lying in the plane of the pyrimidine molecule and the axis perpendicular to the pyrimidine ring, we obtain the two diagonal elements of  $\underline{\underline{\alpha}}$  which are necessary for a rotation of a magnetic field  $H$  in the *ac*-plane.